

1 **PEGylated and poloxamer-modified chitosan nanoparticles incorporating a**  
2 **lysine-based surfactant for pH-triggered doxorubicin release**

3  
4  
5  
6  
7  
8 Laís E. Scheeren<sup>1,2</sup>, Daniele R. Nogueira<sup>1,2,\*</sup>, Letícia B. Macedo<sup>1,2</sup>, M. Pilar Vinardell<sup>3</sup>,  
9 Montserrat Mitjans<sup>3</sup>, M. Rosa Infante<sup>4</sup>, Clarice M. B. Rolim<sup>1,2</sup>

10  
11  
12  
13  
14 <sup>1</sup>*Departamento de Farmácia Industrial, Universidade Federal de Santa Maria, Av. Roraima*  
15 *1000, 97105-900, Santa Maria, RS, Brazil*

16 <sup>2</sup>*Programa de Pós-Graduação em Ciências Farmacêuticas, Universidade Federal de Santa*  
17 *Maria, Av. Roraima 1000, 97105-900, Santa Maria, RS, Brazil*

18 <sup>3</sup>*Departament de Fisiologia, Facultat de Farmàcia, Universitat de Barcelona, Av. Joan XXIII*  
19 *s/n, 08028, Barcelona, Spain*

20 <sup>4</sup>*Departamento de Tecnología Química y de Tensioactivos, IQAC, CSIC, C/ Jordi Girona 18-*  
21 *26, 08034, Barcelona, Spain*

22  
23  
24  
25  
26 \* *Corresponding author: Phone: +55 55 3220 9548; Fax: +55 55 3220 8248*

27 *E-mail address: daniele.rubert@gmail.com (Daniele Rubert Nogueira).*

## 28 **ABSTRACT**

29 The growing demand for efficient chemotherapy in many cancers requires novel approaches in  
30 target-delivery technologies. Nanomaterials with pH-responsive behavior appear to have  
31 potential ability to selectively release the encapsulated molecules by sensing the acidic tumor  
32 microenvironment or the low pH found in endosomes. Likewise, polyethylene glycol (PEG)-  
33 and poloxamer-modified nanocarriers have been gaining attention regarding their potential to  
34 improve the effectiveness of cancer therapy. In this context, DOX-loaded pH-responsive  
35 nanoparticles (NPs) modified with PEG or poloxamer were prepared and the effects of these  
36 modifiers were evaluated on the overall characteristics of these nanostructures. Chitosan and  
37 tripolyphosphate were selected to form NPs by the interaction of oppositely charged  
38 compounds. A pH-sensitive lysine-based amphiphile (77KS) was used as a bioactive adjuvant.  
39 The strong dependence of 77KS ionization with pH makes this compound an interesting  
40 candidate to be used for the design of pH-sensitive devices. The physicochemical  
41 characterization of all NPs has been performed, and it was shown that the presence of 77KS  
42 clearly promotes a pH-triggered DOX release. Accelerated and continuous release patterns of  
43 DOX from CS-NPs under acidic conditions were observed regardless of the presence of PEG  
44 or poloxamer. Moreover, photodegradation studies have indicated that the lyophilization of NPs  
45 improved DOX stability under UVA radiation. Finally, cytotoxicity experiments have shown  
46 the ability of DOX-loaded CS-NPs to kill HeLa tumor cells. Hence, the overall results suggest  
47 that these pH-responsive CS-NPs are highly potent delivery systems to target tumor and  
48 intracellular environments, rendering them promising DOX carrier systems for cancer therapy.

49 **Keywords:** chitosan nanoparticles; doxorubicin; *in vitro* release; *in vitro* cytotoxicity; lysine-  
50 based surfactant; pH-sensitivity

## 51 **1. Introduction**

52 Doxorubicin (DOX) is an anthracycline antibiotic commonly used as a chemotherapeutic agent  
53 [1]. Due to its broad-spectrum of antitumor activity, it has been incorporated into several nano-  
54 sized materials, including pH-responsive microgels [2], temperature-responsive micelles [3],  
55 liposomes [4] and polymeric nanoparticles (NPs) [5,6]. DOX antineoplastic effects can occur  
56 by different mechanisms, such as free radical generation, which is well associated with the  
57 cardiotoxicity of anthracyclines [7]. Drug delivery systems have been gaining attention in recent  
58 years as a promising approach to improve cancer treatment and prevent toxicity in healthy  
59 tissues. It is noteworthy that by adding different modifiers, these systems can be designed for  
60 cancer cell-specific targeting as well as for biological, chemical, or physical stimulus response  
61 [8,9].

62         Considering that endosomal pH (~ 6.5 to 5.5) [10] and the tumor extracellular pH (pH<sub>e</sub>  
63 ~ 6.6) are notably lower than those of normal tissue (pH ~ 7.4) [11], pH-sensitive devices have  
64 been widely researched as drug delivery strategies for cancerous diseases [9]. In this context,  
65 our group has paid special attention to a bioactive amino acid-based surfactant derived from  
66 N<sup>α</sup>,N<sup>ε</sup>-dioctanoyl lysine with an inorganic sodium counterion (77KS), which in previous studies  
67 shown pH-responsive properties and low cytotoxicity [12-14]. Therefore, here we selected  
68 77KS as an adjuvant with potential ability to promote the pH-triggered DOX release in the  
69 tumor microenvironment and endosomal compartments (Fig. 1).

70         Chitosan (CS) is a nontoxic, biocompatible and biodegradable polymer that has been  
71 emerging as one of the most promising delivery vehicles for cancer chemotherapy [15].  
72 Chitosan has been widely used for the development of DOX-loaded NPs by simple and mild  
73 preparation techniques [5,16-18]. CS-NPs modified by polyethylene glycol (PEG) are explored  
74 due to the ability of this hydrophilic polymer to prolong the circulation time of nanocarriers in  
75 the blood stream. This mechanism allows NP accumulation in the tumor region via enhanced  
76 permeability and retention (EPR) effect, which, in turn, increases tumor exposure to the

77 encapsulated drug [19-22]. Likewise, Pluronic block copolymers (or non-proprietary name  
78 “poloxamer”) have been studied as biological response modifiers. They are amphiphilic  
79 synthetic polymers with tumor-sensitizing activity in multidrug resistant (MDR) cells, which is  
80 especially attributed to the inhibition of P-glycoprotein [23]. For this reason, it has been reported  
81 that the association of DOX to poloxamer-based formulations potentiates the drug activity  
82 against non-MDR and, especially, MDR tumor cells [24-26].

83 Therefore, the aim of the present study was to prepare PEGylated and poloxamer-  
84 modified CS-NPs incorporating a lysine-based surfactant as a pH-responsive bioactive adjuvant.  
85 The NPs were well characterized and the mathematical modeling of pH-triggered DOX release  
86 profiles was discussed. NP suspensions and lyophilized samples were analyzed regarding their  
87 stability at low temperature and under UVA radiation. Finally, in order to gain preliminary  
88 insights into the role of the modifiers on the antitumor activity of NPs, the cytotoxicity of free  
89 and entrapped drug was assessed by an *in vitro* cell-based assay.

## 90 **2. Materials and methods**

### 91 *2.1. Materials*

92 Chitosan (CS) of low molecular weight (deacetylation degree, 75-85%; viscosity, 20-300 cP  
93 according to the data sheet of the manufacturer), pentasodium tripolyphosphate (TPP),  
94 polyethylene glycol methyl ether (mPEG,  $M_n = 5,000$ ), poloxamer 188 solution (10%, w/v) and  
95 2,5-diphenyl-3-(4,5-dimethyl-2-thiazolyl) and tetrazolium bromide (MTT) were purchased  
96 from Sigma-Aldrich (St. Louis, MO, USA). Reagents for cell culture were from Vitrocell  
97 (Campinas, SP, Brazil). Doxorubicin (DOX, state purity 98.32%) was obtained from Zibo  
98 Ocean International Trade (Zibo, Shangdong, P.R., China). Acetonitrile and glacial acetic acid  
99 were purchased from Tedia (Fairfield, USA). All other solvents and reagents were of analytical  
100 grade.

## 101 2.2. Surfactant included in the nanoparticles

102 An anionic amino acid-based surfactant derived from N<sup>α</sup>,N<sup>ε</sup>-dioctanoyl lysine and with an  
103 inorganic sodium counterion (77KS) was included in the NP formulation. The surfactant  
104 chemical structure is formed by two alkyl chains (each with eight carbon atoms) bound to the  
105 amino acid lysine. It has a molecular weight of 421.5 g/mol and a critical micellar concentration  
106 (CMC) of  $3 \times 10^3$  μg/ml [27,28]. This surfactant was synthesized as described elsewhere [29].

## 107 2.3. Preparation of nanoparticles

108 CS-NPs were spontaneously formed by ionotropic gelation process, according to the  
109 methodology first described by Calvo et al. [30]. DOX stock solution was prepared in ultrapure  
110 water in order to give a final concentration of 2.0 mg/ml. Chitosan at 1.0 mg/ml was dissolved  
111 in a 1.0% (v/v) acetic acid aqueous solution under magnetic stirring for 2 h, and pH was adjusted  
112 to 5.5 with 10 M NaOH [31]. A mixed solution of the cross-linker TPP and the surfactant 77KS  
113 was prepared in ultra-pure water at 2.0 mg/ml and 0.5 mg/ml, respectively. Initially, DOX stock  
114 solution was added to 5 ml of CS solution (CS:DOX ratio 5:0.5, w/w) and maintained under  
115 magnetic stirring (1000 rpm) for 10 min. Then, 1 ml of a premixed TPP:77KS solution (ratio  
116 equal 2:0.5, w/w) was added drop-wise into the CS:DOX solution. NPs (DOX-CS-NPs) were  
117 formed spontaneously and the gelation process was carried out under constant magnetic stirring  
118 for 20 min at room temperature.

119 In order to obtain PEGylated DOX-CS-NPs (PEG-DOX-CS-NPs), a mixed solution of  
120 CS and PEG (at 1 mg/ml and 10 mg/ml, respectively) was prepared in 1.0% (v/v) acetic acid.  
121 To 5 ml of this solution, DOX stock solution was added and stirred for 10 min (CS:PEG:DOX  
122 ratio 5:50:0.5, w/w/w). Afterwards, 1 ml of TPP:77KS (2:0.5, w/w) was added drop-wise and  
123 stirred for 20 min.

124 Poloxamer-modified DOX-CS-NPs (Polox-DOX-CS-NPs) were obtained by adding  
125 0.5% (w/v) of poloxamer to 5 ml of a 1 mg/ml CS solution. Next, DOX stock solution was  
126 added to give a final ratio of CS:Poloxamer:DOX 5:25:0.5 (w/w/w). Finally, 1 ml of TPP:77KS  
127 (2:0.5, w/w) was added drop-wise under vigorous magnetic stirring for 20 min.

128 Unloaded NPs were prepared similarly for each formulation, thus omitting the drug. All  
129 procedures involving DOX were conducted in a low incidence of light. The resulting DOX-  
130 loaded NPs were purified by dialysis for 1 h in distilled water (dialysis bag - Sigma-Aldrich,  
131 14,000 MWCO), in order to remove the non-encapsulated drug and non-incorporated  
132 constituents.

#### 133 *2.4. Characterization of nanoparticles*

134 The mean hydrodynamic diameter and the polydispersity index (PDI) of the NPs were  
135 determined by dynamic light scattering (DLS) using a Malvern Zetasizer ZS (Malvern  
136 Instruments, Malvern, UK), without any dilution of the samples. The zeta potential (ZP) values  
137 of the NPs were assessed by determining electrophoretic mobility using the same equipment  
138 after dilution of the formulations in 10 mM NaCl aqueous solution (1:10 volume per volume).  
139 Each measurement was performed using at least three sets of ten runs at 25°C. The pH  
140 measurements were verified directly in the NP suspensions, using a calibrated potentiometer  
141 (UB-10; Denver Instrument, Bohemia, NY, USA), at room temperature. Finally, the spectral  
142 properties of the drug were assessed before its encapsulation and also after extraction from the  
143 NP structure. This assay was performed in order to verify the stability of DOX after entrapment  
144 into the NP matrix. Experiments were performed on a double-beam UV-Vis spectrophotometer  
145 (Shimadzu, Japan) model UV-1800, with a fixed slit width (2 nm) and a 10 mm quartz cell was  
146 used to obtain spectrum and absorbance measurements. The diluent optimized was water pH  
147 3.0, acidified with glacial acetic acid.

148 *2.5. Drug encapsulation efficiency*

149 The quantitative analyses were performed by a reversed-phase liquid chromatography (RP-LC)  
150 method that was previously validated according to international guidelines and proved to be  
151 specific, linear, precise, accurate and robust (unpublished data). Chromatographic analyses were  
152 carried out on a LC 1260 Agilent Technologies system (Agilent Technologies, Santa Clara, CA,  
153 USA), using a Waters XBridge™ C18 column (250 mm x 4.6 mm I.D., 5µm), with a mobile  
154 phase consisting of 90% (v/v) acetonitrile in water and water pH 3.0, acidified with glacial acetic  
155 acid (33:67, v/v) and UV detection set at 254 nm. Data analysis was performed with EZChrom  
156 software program (version A.01.05). Total drug content was achieved by dilution of the NP  
157 suspensions in methanol (1:1, v/v) followed by sonication for 15 min, which allowed total drug  
158 extraction from the NP matrix. The resulting solution was diluted to the suitable concentration  
159 and analyzed by RP-LC. The drug association efficiency was determined by  
160 ultrafiltration/centrifugation technique using Amicon Ultra-0.5 Centrifugal Filters (10,000 Da  
161 MWCO, Millipore). An amount of the non-purified NP suspension was placed into this device  
162 and submitted to 10,000 rpm for 20 min in a Sigma 2-16P Centrifuge (Sigma, Germany). The  
163 encapsulation efficiency (EE%) was calculated as the difference between total and free DOX  
164 concentrations determined in the NP suspension (total drug content) and in the ultrafiltrate,  
165 respectively, using the mentioned analytical method.

166 *2.6. pH-dependent in vitro DOX release*

167 *In vitro* release assessments of DOX from the different CS-NPs were performed using the  
168 dialysis method. An aliquot of the NPs (1 ml) was placed into a dialysis bag (Sigma-Aldrich,  
169 14,000 MWCO), which was immersed in 50 ml of phosphate buffered saline (PBS) at 37°C and  
170 kept under gentle magnetic stirring (100 rpm) for 24 h. This process was carried out, separately,  
171 in PBS at pH 7.4, 6.6 and 5.4. At specific time intervals, an aliquot of 2 ml of the external

172 medium was withdrawn and filtered through a 0.45- $\mu\text{m}$  membrane. Thereafter, equal volume of  
173 fresh buffer was added to maintain the sink conditions and constant volume. The release of the  
174 free drug was also investigated in the same way. The released amount of DOX in each scheduled  
175 time was estimated by the RP-LC method described in the previous section (*section 2.5*), using  
176 analytical curves obtained with the release medium (PBS at pH 7.4, 6.6 or 5.4) as diluents. The  
177 cumulative release percentage (CR%) of DOX was determined from the following equation (Eq.  
178 (1)):

$$179 \quad CR\% = (M_t/M_i) 100 \quad (1)$$

180 where  $M_t$  and  $M_i$  are the amount of drug released at the time  $t$  and the initial amount of drug  
181 encapsulated in the NPs, respectively. The *in vitro* release studies were carried out in triplicate.

182 For understanding the pH-sensitivity behavior of NPs, swelling studies were performed  
183 by soaking lyophilized NPs into PBS pH 7.4, 6.6 and 5.4 at room temperature and under gentle  
184 shake. Hydrodynamic diameter was measured after 3 h incubation.

### 185 *2.7. Mathematical modeling of drug release profiles*

186 Monoexponential (Eq. (2)) and biexponential (Eq. (3)) mathematical models as well as the  
187 Korsmeyer-Peppas model (Eq. (4)) were used to analyze DOX *in vitro* release profile  
188 (MicroMath® Scientist version 2.01, USA). The model that best fit the drug release profile was  
189 selected according to the model selection criteria (MSC), correlation coefficient ( $r$ ), and  
190 graphical adjustment. The release kinetic rate constants are  $k$  (for monoexponential),  $k_1$  and  $k_2$   
191 (for biexponential).  $C_0$ ,  $a$  and  $b$  are the initial concentration for mono- and biexponential models,  
192 respectively [32,33]. Finally, the DOX release mechanism was investigated by fitting 60% of  
193 the initial amount of drug released from CS-NPs to the Korsmeyer-Peppas model. In its  
194 corresponding equation,  $n$  is the exponent that characterizes the release mechanism and  $a$  is a  
195 constant comprising the structural and geometric characteristics of the carrier [34-36].

196  $C = C_0 e^{-kt}$  (2)

197  $C = a e^{-k_1 t} + b e^{-k_2 t}$  (3)

198  $ft = a t^n$  (4)

199 *2.8. Lyophilization of nanoparticles*

200 NP suspensions DOX-CS-NPs, PEG-DOX-CS-NPs and Polox-DOX-CS-NPs were subjected to  
201 the lyophilization process to obtain dried formulations (L-DOX-CS-NPs, L-PEG-DOX-CS-NPs  
202 and L-Polox-DOX-CS-NPs, respectively). To avoid possible particle aggregation, glycerol  
203 (10%, w/v), mannitol (1%, w/v) and lactose (1, 5 and 10%, w/v) were tested for their  
204 cryoprotectant efficiency. Cryoprotectants were dissolved in the entire volume of NPs under  
205 magnetic stirring for 20 min. Then, these mixtures were frozen at -20°C for 48 h. The water was  
206 removed from frozen NPs by sublimation under vacuum for 48 h using a bench top lyophilizer  
207 (Liotop L101, Liobras, São Carlos, Brazil). As required, lyophilized products were redispersed  
208 with ultra-pure water by magnetic stirring for 10 min. The macroscopic appearance,  
209 physicochemical properties and EE% were evaluated.

210 *2.9. Fourier Transform Infrared Spectroscopy (FT-IR) analysis*

211 In order to investigate the interactions between the drug and NP matrix, **FT-IR spectra of dried**  
212 **NPs, pure DOX, CS and 77KS raw materials** were recorded using compressed KBr disk method  
213 with a FT-IR spectrophotometer (Bruker Tensor 27, Bruker Optik, Ettlingen, Germany).  
214 Spectral acquisition was carried out from 4000 to 400 cm<sup>-1</sup> range.

215 *2.10. Stability studies of nanoparticles*

216 NP suspensions (DOX-CS-NPs, PEG-DOX-CS-NPs and Polox-DOX-CS-NPs) and the  
217 lyophilized formulations (L-DOX-CS-NPs and L-PEG-DOX-CS-NPs) were studied for their

218 stability in low temperature (2 – 8°C). Experiments were conducted over 8 weeks. Lyophilized  
219 samples were first placed inside a desiccator containing silica and then exposed to low  
220 temperature whilst protected from light. Analyses were carried out on the first day of the study,  
221 and subsequently after 2, 4 and 8 weeks. In each time point, all samples were evaluated for  
222 particle size, PDI, ZP and drug content (total drug amount (%) in regard to freshly prepared  
223 formulations).

224 Additionally, photostability studies were carried out to assess whether suspensions  
225 and/or lyophilized formulations were able to protect the drug after exposure to UVA radiation.  
226 An aliquot of DOX solution or DOX-loaded NPs was put separately into transparent capped  
227 cuvettes (Brand®, UV-Cuvettes micro) and placed into a mirrored chamber with approximately  
228 1,350 W h/m<sup>2</sup> incident UVA radiation [37]. On the other hand, an amount of the lyophilized  
229 formulations were weighed and well distributed in Petri dishes. The drug concentration was  
230 measured in different schedule times (0, 2, 8, 24 and 48 h) by the validated RP-LC method.  
231 Zero, first and second order graphics were delineated and the one with the best fit was  
232 considered to establish the kinetic order.

### 233 2.11. Cytotoxicity assays

234 The *in vitro* antitumor activity of unloaded-CS-NPs, DOX-loaded CS-NPs and free DOX was  
235 determined against HeLa cell line (human epithelial cervical cancer), which was cultured in  
236 DMEM medium (4.5 g/l glucose) supplemented with 10% (v/v) FBS, at 37°C in a 5% CO<sub>2</sub>  
237 atmosphere. HeLa cells were seeded into 96-well cell culture plates at a density of 7.5 x 10<sup>4</sup>  
238 cells/ml. Cells were incubated for 24 h under 5% CO<sub>2</sub> at 37°C and afterwards, the medium was  
239 replaced with 100 µl of fresh medium containing the treatments. Free DOX as well as DOX-  
240 loaded CS-NPs were assayed at 1 and 10 µg/ml DOX concentration, while unloaded CS-NPs  
241 were assessed at 50 and 200 µg/ml. Following 24 h incubation, the medium was removed and

242 100 µl of MTT in PBS (5 mg/ml) diluted 1:10 in medium without FBS was added to the cells  
243 and incubated for 3 h. Finally, the MTT containing medium was removed and 100 µl of DMSO  
244 was added to each well in order to dissolve the purple formazan product. After shaking, the  
245 absorbance of the resulting solution was measured using a SpectraMax M2 (Molecular Devices,  
246 Sunnyvale, CA, USA) microplate reader at 550 nm. Cell viability was calculated as the  
247 percentage of tetrazolium salt reduced by viable cells in each sample. The untreated cell control  
248 (cells with medium only) was taken as 100% viability.

#### 249 *2.12. Statistical analyses*

250 Results are expressed as mean ± standard error (SE) or mean ± standard deviation (SD) of three  
251 independent experiments, and statistical analyses were performed using one-way analysis of  
252 variance (ANOVA) to determine the differences between the datasets, followed by Tukey's  
253 post-hoc test for multiple comparisons, using SPSS<sup>®</sup> software (SPSS Inc., Chicago, IL, USA).  
254  $p < 0.05$  and  $p < 0.01$  indicated significant and highly significant differences, respectively.

### 255 **3. Results and discussion**

256 In this study, NPs encapsulating DOX were prepared by combination of the standard ionotropic  
257 gelation method [30] and the inclusion of procedures deliberated by our research group.  
258 Therefore, novel pH-responsive CS-NPs were obtained using a mild and solvent-free process  
259 for efficient drug loading [38]. CS is widely regarded as being a non-toxic and biologically  
260 compatible polymer, with great medical potential [39]. Once dissolved in acetic acid aqueous  
261 solution, the amino groups of CS are protonated ( $\text{NH}_3^+$ ) and available to interact with the  
262 negatively charged TPP ( $\text{P}_3\text{O}_{10}^{5-}$ ) to spontaneously form the NPs [40,41]. With the aim to find  
263 the suitable CS:TPP ratio (w/w), different TPP concentrations were tested since the size and  
264 PDI of NPs depended on the amount of TPP in the formulation. The first condition tested was  
265 CS:TPP (5:1, w/w), but the ratio CS:TPP (5:2, w/w) was chosen since it presented the smallest

266 size and PDI value. This behavior can be attributed to the greater interaction of CS positive  
267 charges with increasing amount of negative charges of the polyanion TPP [42]. These results  
268 are in agreement with the study reported by Gan et al. [43], in which a linear decrease of size  
269 with decreasing CS to TPP weight ratio was observed. Furthermore, it is worth pointing out that  
270 by increasing the amount of negative charges into the formulation matrix, the free positive  
271 charges of CS were reduced. This lower protonation diminishes the repulsion between CS and  
272 DOX (also positively charged), which, in turn, increases the drug encapsulation efficiency.

273         The surfactant 77KS was selected as a bioactive adjuvant in the NP formulation based  
274 on previous studies, which showed its pH-sensitive activity along with improved kinetics in the  
275 endosomal pH range and low cytotoxic potential [12,13]. Moreover, it was already  
276 demonstrated that the inclusion of another amphiphile from the same family (77KL, with lithium  
277 counterion) in the composition of polymeric NPs improved their *in vitro* antitumor activity and  
278 also gave them a pH-responsive behavior [44]. The surfactant 77KS was included into the NPs  
279 at a concentration below its CMC, indicating that it is present in the formulations in the  
280 monomer form. Different concentrations of the surfactant were tested, ranging from  
281 CS:TPP:77KS 5:2:0.1 to 5:2:1 (w/w/w), with 0.1 increase amount of 77KS each time. By having  
282 the concentration ratio of 77KS higher than 5:2:0.5, a flocculation of the NPs took place. In  
283 contrast, concentrations between 0.1 and 0.5 provided satisfactory results. Therefore, the ratio  
284 5:2:0.5 (w/w/w) of CS:TPP:77KS was chosen and maintained for all formulations.

285         The process to prepare the NPs was optimized to be simple and fast. Firstly, positive  
286 charges (DOX and CS) were mixed [5,17] and, a premixed solution of the negatively charged  
287 compounds (TPP and 77KS) was added drop-wise, leading to spontaneous formation of the  
288 colloidal system. It is known that the polyanion TPP has multiple charged functional groups,  
289 which makes it able to interact with both DOX and CS, resulting in shielding and electrostatic  
290 interactions [17]. The pH of CS solution was set at 5.5, in which about 90% of the amino groups

291 of CS ( $pK_a = 6.5$ ) are protonated [45]. Likewise, DOX ( $pK_a = 8.2$ ) possess an amino sugar  
292 moiety also protonated at this pH [46], which allowed competitive binding of DOX to the  
293 negatively charged cross-linking agent (TPP) while forming the NPs.

294 The PEGylation of nanomaterials was shown not only to diminish clearance of the  
295 loaded drug, but also to provide enhanced tumor targeting ability due to the prolongation of  
296 plasma circulation time [47]. PEGylated DOX-CS-NPs were prepared from CS and PEG joint  
297 solubilization prior to gelation process, where a CS/PEG network is formed by cross-linking  
298 between hydroxyl groups of PEG and amino groups of CS [48]. Likewise, it is known that block  
299 copolymers, such as the poloxamers, are biological response modifiers with potential ability to  
300 modulate drug resistance in MDR cancer cells. Therefore, here poloxamer-modified DOX-CS-  
301 NPs were prepared upon the addition of TPP:77KS into CS:Poloxamer:DOX solution [49].  
302 Different concentrations of poloxamer were tested (0.2%, 0.5% and 1%, w/v), and the  
303 intermediate one (0.5%) was chose with acceptable physicochemical characteristics. It was  
304 previously reported that micelles containing block copolymers at 0.25 and 2% (w/v), in which  
305 DOX is also non-covalently incorporated, exhibited greater efficacy than free DOX in *in vitro*  
306 and *in vivo* tumor models [50].

### 307 3.1. Characterization and EE% of nanoparticles

308 Following the preparation procedure, the stability of the drug after its encapsulation was  
309 assessed through the spectral analysis, as shown in Fig. 2. The UV-Vis spectrum of the drug  
310 extracted from NPs was similar to that obtained for DOX in free solution, which proved the  
311 integrity of DOX molecule after its entrapment into the NP matrix. Moreover, as summarized  
312 in Table 1, DOX-loaded and unloaded NPs were characterized for particle size, PDI, ZP and  
313 pH. The average particle size analysis is a common characterization method, which allows the  
314 understanding of their dispersion and aggregation, as well as helping to predict their possible

315 biodistribution. The size of unloaded NPs was in the range of 170 to 211 nm. Increasing  
316 diameters were noticed when DOX was added, indicating the retention of the drug. Likewise,  
317 the mean diameter of PEGylated NPs increased with respect to unmodified NPs, which is a good  
318 indicator of PEG incorporation into the NP structure [22]. Here, it can be stated that PEG was  
319 incorporated into the colloidal gel system via hydrogen bonding between the oxygen atom of  
320 PEG and amino groups of CS. This interaction is weak, which makes the structure of the  
321 PEGylated NPs looser and, consequently, increases their mean diameter [20]. Conversely,  
322 poloxamer-modified NPs presented smaller mean diameter than those PEG-modified NPs. This  
323 is due to the stabilizer power of poloxamer, fact that leads to a rigid arrangement of particles  
324 with less water uptake [49]. Additionally, all CS-based NPs formed systems with narrow size  
325 distribution with PDI values lower than 0.24. The ZP values of the NPs in the range of 21 to 25  
326 mV indicate a positively charged surface owing to the cationic amino groups of CS. Likewise,  
327 when DOX was present, the electric charge remained positive and no considerable changes were  
328 noted.

329 DOX-loaded NPs displayed high EE% and the mean values obtained for all formulations  
330 were constantly around 65%. These results are in agreement with those found elsewhere [22,51],  
331 and allow us to state that the drug was entrapped into the polymeric network regardless of  
332 modifications made in NPs. Indeed, different amounts of drug loading were tested and discussed  
333 based on EE% capacity. By increasing DOX concentration from 80 to 154  $\mu\text{g/ml}$ , the DOX  
334 EE% decreased from  $66.50\% \pm 2.68$  to  $51.09\% \pm 2.88$ . Similar results were found elsewhere  
335 [17,18,52], pointing out that a larger amount of drug does not mean any increase in  
336 encapsulation efficiency. As a limited number of functional groups is available for electrostatic  
337 interactions with the drug in the NP matrix, the increase in the amount of drug added to the  
338 formulation could have resulted in a decrease in drug entrapment efficiency. Finally, it is worthy  
339 mentioning that NPs without 77KS showed the highest mean EE% value. This behavior could

340 be attributed to the assembling of a consistent CS/TPP network with greater amount of TPP  
341 molecules and, thus, of remaining negative charges that allow DOX association. When 77KS  
342 (with only one negatively charged group) binds to CS, no free negative charge remains available  
343 to interact with DOX, therefore leading to diminished EE%. However, it is important to  
344 highlight that when 77KS was incorporated, we achieved higher EE% values than previous  
345 studies that reported DOX EE% values in the order of 47% for PLGA NPs and 20% for CS-  
346 based NPs [5,53].

### 347 3.2. *In vitro* DOX release

348 Taking advantage of the acidic pH<sub>e</sub> (6.5 – 7.2) found in the tumor environment compared to the  
349 normal tissues [11,54], pH-sensitive NPs have been developed to achieve accelerated drug  
350 release at the tumor site. In this context, the *in vitro* drug release profiles of DOX-CS-NPs, PEG-  
351 DOX-CS-NPs and Polox-DOX-CS-NPs were studied in PBS buffer mediums at pH 7.4, 6.6 and  
352 5.4 at 37 ± 2°C (Fig. 3).

353 When 77KS was first studied, it demonstrated pH-dependent membrane-lytic activity on  
354 hemolysis assay, with significant increase at pH 5.4; although with no pharmaceutical  
355 applications up to this time [13]. Here, this surfactant was incorporated into DOX-loaded CS-  
356 based NPs and, as can be seen in Fig. 3A, it was clearly demonstrated that the pH-dependent  
357 release pattern of these nanostructures was as evident as was for CS-NPs without 77KS (Fig.  
358 3D). In acidic environment, the release rate was accelerated; with 97 and 100% of DOX released  
359 at pH 6.6 and 5.4 after 6 h, respectively, while only 71% of drug release was reached at pH 7.4.  
360 The cumulative release amount of DOX at pH 6.6 and 5.4 was in general significantly faster (p  
361 < 0.05) than at pH 7.4. A control experiment using free DOX was also carried out under similar  
362 conditions and almost total drug release was reached after 6 h.

363 The release of PEG-DOX-CS-NPs was also studied at different pH values, wherein at  
364 acidic conditions the release was noticeably accelerated with 100% of the DOX available in  
365 both pH 6.6 and 5.4 mediums after only 4 h (Fig. 3B). These results demonstrate that PEG did  
366 not inhibit drug release at acidic conditions, which is particularly important in order to maintain  
367 the improved drug delivery in the tumor microenvironment and intracellular compartments.  
368 Unexpectedly, DOX release from PEGylated NPs was not delayed at physiological pH in  
369 comparison with those NPs without PEG (~75 and 76% DOX released at 24 h, respectively).  
370 This behavior appears to be attributed to the formation of a semi-interpenetrating network  
371 between CS and PEG [48] and not to the assembly of a PEG shell around the NPs.

372 Among the three formulations, Polox-DOX-CS-NPs was the one that presented faster  
373 release rate: release amount of DOX reached 100% after 3 h, 5 h and 8 h at pH 5.4, 6.6 and 7.4,  
374 respectively (Fig. 3C). This behavior may be explained by the hydrophilic pattern of poloxamer  
375 that consequently forms a porous structure in the surface of the DOX-CS-NPs [55]. Poloxamers  
376 are reported to be pore-forming agents and drug-releasing enhancers [56], which corroborated  
377 our results. At this point there is no significant difference among the release rates at each pH ( $p$   
378  $> 0.05$ ), which may be justified by the faster release achieved at physiological conditions.

379 The release mechanisms from CS-based NPs have been reported to be desorption of the  
380 drug from the surface, diffusion of the drug through pores, and degradation of the polymeric  
381 matrix [43]. In the swelling experiments, a considerable increase of particle size was noticed  
382 with a decrease of the buffer pH from 7.4 and 6.6 to 5.4 (178.9 nm, 173.6 nm and 309.7 nm,  
383 respectively). At lower pH value, the protonation of the amino groups of CS is promoted,  
384 leading to an increase of electric density and repulsion force between cross-linked CS chains  
385 [57]. This mechanism allows the medium to penetrate into the nanoparticulate system,  
386 consequently increasing the mean hydrodynamic size [58]. This pH-sensitive swelling behavior,  
387 in turn, could be one of the mechanisms underlying the faster diffusion of DOX from NPs,

388 especially in acidic environments with pH as low as 5.4. On the other hand, the lack of swelling  
389 at pH 6.6 is probably attributed to the diminishing CS protonation in this condition, suggesting  
390 that the repulsion forces are not enough to induce NP swelling and, thus, other mechanisms are  
391 involved in the accelerated drug release.

392 It is worth mentioning that besides the swelling mechanism of CS, DOX may have an  
393 improved solubility and, TPP, a reduced ionization in acidic environments [17,57]. This later  
394 condition may result in NP network destabilization and thus faster drug delivery, which could  
395 be the basis for the pH-responsive drug release observed for the NPs without 77KS (Fig. 3D).  
396 Considering that either CS-NPs with or without 77KS displayed a pH-dependent release  
397 behavior, it can be evidenced that the pH-responsive nature of CS itself appears to play the  
398 dominant role. However, 77KS appears to delay the release at pH 7.4, which is quite important  
399 in order to achieve a target drug release at the tumor site. Therefore, it can be stated that 77KS  
400 has a synergic effect with CS to give to the NPs the pH-responsive behavior. Moreover, it is  
401 noteworthy that another study performed by our research group evidenced that only the NPs  
402 incorporating 77KS showed pH-sensitive membrane-lytic activity (unpublished data), which  
403 also proves the important role of 77KS to improve the pH-sensitivity of the NPs. The ionization  
404 of 77KS is expected to be reduced in an acidic environment [13], which in turn would also  
405 contribute for the destabilization of the NP structure due to the reduced amount of available  
406 anionic charges that interact electrostatically with CS. This process would retain the drug at  
407 physiological conditions and facilitate the drug release as the pH decreases to 6.6 and 5.4.

408 The increased release at pH 6.6 and 5.4 shows that drug delivery appears to be triggered  
409 at tumor extracellular pH<sub>e</sub>, as well as at the acidic environment of endosomes. Moreover, the  
410 low DOX release at normal physiological conditions may reduce the side effects that can occur  
411 during cancer treatment. Altogether, these results support the idea that these nanocarriers are a

412 potential design to be used as a pH-sensitive system to improve the drug availability on tumor  
413 microenvironment and intracellular compartments.

### 414 3.3. Mathematical modeling

415 The data obtained from *in vitro* release studies were used to calculate values of release constants  
416 and release exponents with the aim to help understanding the mathematics of release profiles  
417 (Table 2). According to the values of the correlation coefficients ( $r$ ) and MSC, the data for all  
418 NPs suspensions at pH 7.4 fit better to the biexponential equation ( $r > 0.99$ ). At this condition,  
419 the DOX release showed an initial burst release ( $k_1$ ), continued by a steady-state release ( $k_2$ ).  
420 These two phases can be explained by the initial drug release from NP surface (drug adsorbed  
421 or entrapped in surface layer), followed by buffer penetration into NPs and drug diffusion  
422 through the swollen rubbery matrix [58]. Moreover, according to the results for  $a$  and  $b$   
423 parameters, approximately 68% of the drug was in Polox-DOX-CS-NPs and only 31% was  
424 superficially adsorbed on this nanostructure. Conversely, PEG-DOX-CS-NPs and DOX-CS-  
425 NPs had about 25% encapsulated and 75% adsorbed on NP surface. When the mathematical  
426 modeling was performed for pH 6.6 and 5.4, a good fit was observed using the monoexponential  
427 model, with constant rates ( $k$ ) in the following ranking order: PEG-DOX-CS-NPs > Polox-  
428 DOX-CS-NPs > DOX-CS-NPs.

429 In the Korsmeyer-Peppas model, high correlation coefficient was obtained ( $r > 0.99$  for  
430 NPs and  $r > 0.98$  for free DOX). The values of release exponent ( $n$ ) between 0.43 and 0.85 for  
431 DOX-CS-NPs (release medium at pH 7.4, 6.6 and 5.4, with  $n = 0.6836$ , 0.4608 and 0.5235,  
432 respectively) indicate a non-Fickian-type release mechanism, i.e., the phenomena responsible  
433 for the DOX release are drug diffusion process from the NPs coupled to relaxation of the  
434 polymeric chains [59]. A non-Fickian model also was found for PEG-DOX-CS-NPs at pH 7.4  
435 ( $n = 0.5010$ ) and Polox-DOX-CS-NPs at pH 7.4 and pH 5.4 ( $n = 0.4836$  and 0.6638,

436 respectively). The same mechanism transport was identified for the release of rivastigmine from  
437 CS-based nanoparticles for brain targeting [60]. When the release data of PEG-DOX-CS-NPs  
438 at pH 6.6 and 5.4 mediums were analyzed,  $n < 0.43$  was obtained and, therefore, the release  
439 mechanism was Fickian, suggesting that the release is a consequential effect of only DOX  
440 amount diffused from the nanostructure. The same occurred for Polox-DOX-CS-NPs at pH 6.6.  
441 Fickian release mechanism was also presented to an anticancer drug loaded into CS-NPs [57].  
442 Finally,  $n = 0.2276$  was obtained for non-encapsulated DOX, indicating that its release profile  
443 is diffusion-controlled. Altogether, our results demonstrated the remarkable contribution of the  
444 relaxational process of the polymeric matrix for DOX release at pH 7.4, which may justify the  
445 slower drug release under physiological conditions.

#### 446 *3.4. Lyophilization of nanoparticles*

447 Nanoparticulate systems for drug delivery have been subjected to lyophilization in order to  
448 overcome their instabilities [61]. Herein, NP suspensions were lyophilized by freeze drying with  
449 lactose, mannitol or glycerol as cryoprotectants, which are important adjuvants with the ability  
450 to protect NP suspensions from the stresses generated during the lyophilization process, i.e.  
451 freezing and desiccation [62]. When mannitol and glycerol were tested as protectants, the  
452 obtained result was not satisfactory since the redispersion procedure showed a strong tendency  
453 to form aggregates. For the sake of choosing between 1, 5 and 10% lactose, the major criteria  
454 evaluated were the yield, drug content and redispersibility index (ratio between the size after  
455 lyophilization and before lyophilization). Satisfactory values were achieved for 10% lactose  
456 (~92%, ~93% and 1.10, respectively). Moreover, only 10% lactose was able to produce a clear  
457 suspension, without any visible precipitates (Table 1). Sugars are suitable protective agents,  
458 acting by hydrogen bonding and maintaining the solute in a pseudo hydrated state during the

459 dehydration step, which thus protects the NP structure from damage in dehydration and  
460 rehydration process [63].

### 461 3.5. FT-IR analysis

462 FT-IR analyses were performed in order to support the CS:TPP cross-link as proof of NP  
463 formation, as well as to confirm the grafting of 77KS, PEG and poloxamer on the surface of  
464 NPs (Fig. 4 and 5). Fig. 4B represents the FT-IR spectrum of CS. The characteristic absorption  
465 peak at 3384  $\text{cm}^{-1}$ , representing the presence of OH- groups, indicates that CS is partially  
466 deacetylated. [64]. Peaks at 2850 to 2920  $\text{cm}^{-1}$  show the stretching band of methylene in CS  
467 structure. Moreover, for CS-NPs (Fig. 4C; 5B, C and D), the amino band is shifted from 1652.5  
468 to  $\sim 1570 \text{ cm}^{-1}$ , confirming that amino groups of CS were involved in the cross-linking by  
469 phosphate (TPP) [49]. This shifting was confirmed by analyzing the spectrum of unloaded CS-  
470 NPs (data not showed). Another peak that can be observed in CS-NPs spectra (Fig. 4C; 5B, C  
471 and D) is at 1202  $\text{cm}^{-1}$ , corresponding to P=O stretching of the TPP [64]. Pure DOX spectrum  
472 (Fig. 4A) shows peaks at 2933 (C-H), 1730 (C-O), 1617 and 1582 (N-H), 1413 (C-C) and 1072  
473  $\text{cm}^{-1}$  (C-O). In DOX-CS-NPs spectra (Fig. 4C; 5B, C and D), these peaks are also presented as  
474 shifted to 2900 (C-H), 1642 and 1572 (N-H), 1415(C-C) and 1031  $\text{cm}^{-1}$  (C-O). Thus, these  
475 results indicate that DOX was loaded into CS-NPs [18]. Absorption peaks associated to PEG  
476 can be seen at 784 and 897  $\text{cm}^{-1}$ , suggesting that PEG grafting was successfully achieved in  
477 PEG-DOX-CS-NPs (Fig. 5D) [21]. Likewise, for Polox-DOX-CS-NPs (Fig. 4C), a stretching  
478 band from 2860 to 2950  $\text{cm}^{-1}$  confirms the incorporation of poloxamer 188. The same strong  
479 peak appears for pure poloxamer, which represents the stretching vibrational band of methylene  
480 group [49,65]. Finally, for 77KS, two strong bands at 1550  $\text{cm}^{-1}$  and 1414  $\text{cm}^{-1}$  represents the  
481 carboxylate ion present in the molecule (Fig. 5A) [66]. The peak at  $\sim 1414 \text{ cm}^{-1}$  remains as a  
482 strong band and evidences the incorporation of 77KS in CS-NPs (Fig. 5B and D). For DOX-

483 CS-NPs without 77KS, this band was shifted to  $1423\text{ cm}^{-1}$  and appears with small intensity (Fig.  
484 5C). The band at  $1550\text{ cm}^{-1}$  could not be used to evidence the incorporation of 77KS because it  
485 overlaps with N-H bending vibrations of CS amino groups.

### 486 3.6. Stability studies of nanoparticles

487 NP suspensions and NPs after lyophilization were submitted to stability studies for a storage  
488 period of 8 weeks at  $2 - 8^{\circ}\text{C}$ . Particle size, PDI, ZP and drug content were evaluated in each  
489 scheduled time. After two weeks storage, all samples presented a tendency to aggregate. The  
490 parameters evaluated that prove this fact are particle size ( $> 600\text{ nm}$ ) and PDI ( $> 0.3$ ), suggesting  
491 an increase in the number of larger particles and a decrease in the narrow size distribution of the  
492 suspension. These results were not unexpected, as it was previously reported that CS  
493 microparticles showed reduced ZP and enhanced particle size after 28 days storage [67]. Factors  
494 to explain the size evolution during time storage are swelling, particle aggregation and  
495 interaction of free polymer chains with the particle network [63]. On the other hand, NP  
496 suspensions presented no considerable variations for drug content, which remained around 99%  
497 during storage time. However, the lyophilized NPs displayed a slight decrease in the drug  
498 content after 1-month storage. Altogether, the results obtained in these preliminary studies  
499 indicated that further studies must be conducted in this field in order to improve the stability of  
500 the design formulations.

501 With the aim to study the ability of the nanosystems to protect the encapsulated drug  
502 from photodegradation, DOX water solution, as well as DOX-CS-NPs and PEG-DOX-CS-NPs  
503 in both suspension and lyophilized states were exposed to UVA radiation. DOX water solution  
504 followed a first kinetic order ( $r = 0.9857$ ), with half-live ( $t_{1/2}$ ) = 9.15 h. Likewise, the degradation  
505 profiles of DOX into DOX-CS-NPs and PEG-DOX-CS-NPs were according to a first ( $r =$   
506  $0.9374$ ) and second kinetic order ( $r = 0.9818$ ), with  $t_{1/2} = 4.17\text{ h}$  and  $5.57\text{ h}$ , respectively. These

507 findings of  $t_{1/2}$ , therefore, revealed that the nanostructured systems were not able to protect DOX  
508 from the UVA radiation during the entire study period. In contrast, the lyophilized samples L-  
509 DOX-CS-NPs and L-PEG-DOX-CS-NPs followed a second kinetic degradation order ( $r =$   
510 0.9975 and 0.9950, respectively) and presented encouraging results about  $t_{1/2}$ . L-DOX-CS-NPs  
511 and L-PEG-DOX-CS-NPs demonstrated  $t_{1/2}$  values 15- and 7.5-fold greater (62.5 h and 41.67 h)  
512 compared to their suspension forms, respectively, suggesting an improvement on photostability  
513 of dry solid forms.

### 514 3.7. Cytotoxicity assays

515 *In vitro* assays are very attractive due to ethical aspects and for being a rapid and effective  
516 pathway to assess toxicological responses of new nanotechnologies before going to *in vivo*  
517 studies. Therefore, here we performed a preliminary study on the potential antitumor activity of  
518 the pH-responsive DOX-loaded NPs using an *in vitro* cell model. The cytotoxic responses of  
519 unloaded CS-NPs, DOX-loaded CS-NPs and free DOX were evaluated against HeLa tumor  
520 cells using MTT viability assay. A dose-dependent effect for all formulations tested can be seen  
521 in Fig. 6. The results obtained with DOX-loaded NPs were compared to those with free DOX  
522 in order to ensure that the drug encapsulation improves or at least maintains the cytotoxic effects  
523 of DOX. The *in vitro* antitumor activity of modified and unmodified DOX-loaded NPs was  
524 generally higher than that of free DOX at both tested concentrations. Finally, the cell viability  
525 was higher than 85% at both tested concentrations of unloaded CS-NPs, indicating that the  
526 surfactant 77KS did not promote significant cytotoxic effects [12].

## 527 4. Conclusions

528 In this work, we prepared and characterized PEGylated and poloxamer-modified DOX-CS-NPs  
529 incorporating the pH-sensitive lysine-based surfactant 77KS. NPs showed nanoscale size with  
530 relatively high EE%, whereas an improvement on DOX photostability was noticed when NPs

531 were into dry solid forms. All formulations displayed pH-triggered DOX release and can be  
532 stated as switching nanodevices in release kinetics, ranging from slow drug delivery while  
533 circulating (pH 7.4) to rapid release kinetics once target sites have been reached (pH 6.6 to 5.4).  
534 Finally, cytotoxicity experiments showed the ability of DOX-loaded CS-NPs to kill HeLa tumor  
535 cells. However, further studies in MDR cancer cells are needed to enhance our knowledge  
536 regarding the role of poloxamer together with 77KS in the sensitization of tumor cells.  
537 Altogether, our findings suggested that the pH-responsive DOX-loaded CS-NPs developed here  
538 could be potential stimulus-responsive drug delivery systems to target cancer cells by triggering  
539 the acidic tumor microenvironment as well as endosomal compartments.

#### 540 **Conflict of interest statement**

541 The authors state that they have no conflict of interest.

#### 542 **Acknowledgments**

543 This research was supported by Projects 447548/2014-0 and 401069/2014-1 of the *Conselho*  
544 *Nacional de Desenvolvimento Científico e Tecnológico* (CNPq - Brazil), 2293-2551/14-0 of  
545 *Fundação de Amparo à Pesquisa do Estado do Rio Grande do Sul* (FAPERGS - Brazil) and  
546 MAT2012-38047-C02-01 of the *Ministerio de Economía y Competitividad* (Spain) and FEDER  
547 (European Union). Laís E. Scheeren and Daniele R. Nogueira thank FAPERGS and PNPD-  
548 CAPES (Brazil) for the Masters' and Postdoctoral fellowships, respectively.

549

550 **References**

- 551 [1] P. Vejpongsa, E.T.H. Yeh, *JAAC* 64 (2014) 938-945.  
552 <http://dx.doi.org/10.1016/j.jacc.2014.06.1167>
- 553 [2] M. Dadsetan, K.E. Taylor, C. Yong, Z. Bajzer, L. Lu, M.J. Yaszemski, *Acta Biomater.* 9  
554 (2013) 5438-5446. <http://dx.doi.org/10.1016/j.actbio.2012.09.019>
- 555 [3] J. Akimoto, M. Nakayama, T. Okano, *J. Control. Release* 193 (2014) 2-8.  
556 <http://dx.doi.org/10.1016/j.jconrel.2014.06.062>
- 557 [4] J. Yahuafai, T. Asai, G. Nakamura, T. Fukuta, P. Siripong, K. Hyodo, H. Ishihara, H.  
558 Kikuchi, N. Oku, *J. Control. Release* 192 (2014) 167-173.  
559 <http://dx.doi.org/10.1016/j.jconrel.2014.07.010>
- 560 [5] K.A. Janes, M.P. Fresneau, A. Marazuela, A. Fabra, M.J. Alonso, *J. Control. Release* 73  
561 (2001) 255-267. [doi:10.1016/S0168-3659\(01\)00294-2](https://doi.org/10.1016/S0168-3659(01)00294-2)
- 562 [6] M. Li, Z. Tang, S. Lv, W. Song, H. Hong, X. Jing, Y. Zhang, X. Chen, *Biomaterials* 35  
563 (2014) 3851-3864. <http://dx.doi.org/10.1016/j.biomaterials.2014.01.018>
- 564 [7] D.A.A. Gewirtz, *Biochem. Pharmacol.* 57 (1999) 727-741. [doi:10.1016/S0006-  
565 2952\(98\)00307-4](https://doi.org/10.1016/S0006-2952(98)00307-4)
- 566 [8] H. Ye, A.A. Karim, X.J. Loh, *Mat. Sci. Eng. C* 45 (2014) 609-619.  
567 <http://dx.doi.org/10.1016/j.msec.2014.06.002>
- 568 [9] J. Liu, Y. Huang, A. Kumar, A. Tan, S. Jin, A. Mozhi, X. Liang, *Biotechnol. Adv.* 32 (2014)  
569 693-710. <http://dx.doi.org/10.1016/j.biotechadv.2013.11.009>
- 570 [10] E.S. Lee, K.T. Oh, D. Kim, Y.S. Youn, Y.H. Bae, *J. Control. Release* 123 (2007) 19-26.  
571 [doi:10.1016/j.jconrel.2007.08.006](https://doi.org/10.1016/j.jconrel.2007.08.006)
- 572 [11] L. Tian, Y.H. Bae, *Colloids Surf. B: Biointerfaces* 99 (2012) 116-126.  
573 [doi:10.1016/j.colsurfb.2011.10.039](https://doi.org/10.1016/j.colsurfb.2011.10.039)
- 574 [12] D.R. Nogueira, M. Mitjans, M.R. Infante, M.P. Vinardell, *Int. J. Pharm.* 420 (2011) 51-58.  
575 [doi:10.1016/j.ijpharm.2011.08.020](https://doi.org/10.1016/j.ijpharm.2011.08.020)
- 576 [13] D.R. Nogueira, M. Mitjans, M.R. Infante, M.P. Vinardell, *Acta Biomater.* 7 (2011) 2846-  
577 2856. [doi:10.1016/j.actbio.2011.03.017](https://doi.org/10.1016/j.actbio.2011.03.017)
- 578 [14] D.R. Nogueira, L.B. Macedo, L.E. Scheeren, M. Mitjans, M.R. Infante, C.M.B. Rolim,  
579 M.P. Vinardell, *J. Appl. Biopharm. Pharmacokinet.* 2 (2014) 59-67. [doi:  
580 http://dx.doi.org/10.14205/2309-4435.2014.02.02.3](https://doi.org/10.14205/2309-4435.2014.02.02.3)

- 581 [15] M. Prabakaran, *Int. J. Biol. Macromol.* 72 (2015) 1313-1322.  
582 <http://dx.doi.org/10.1016/j.ijbiomac.2014.10.052>
- 583 [16] S. Mitra, U. Gaur, P.C. Ghosh, A.N. Maitra, *J. Control. Release* 74 (2001) 317-323.  
584 [doi:10.1016/S0168-3659\(01\)00342-X](https://doi.org/10.1016/S0168-3659(01)00342-X)
- 585 [17] T. Ramasamy, T.H. Tran, H.J. Cho, J.H. Kim, Y.I. Kim, J.Y. Jeon, H. Choi, C.S. Yong,  
586 J.O. Kim, *Pharm. Res.* 31 (2013) 1302-1314. doi:10.1007/s11095-013-1251-9
- 587 [18] G. Unsoy, R. Khodadust, S. Yalcin, P. Mutlu, U. Gunduz, *Eur. J. Pharm. Sci.* 62 (2014)  
588 243-250. <http://dx.doi.org/10.1016/j.ejps.2014.05.021>
- 589 [19] A. Gabizon, H. Shmeeda, T. Grenader, *Eur. J. Pharm. Sci.* 45 (2012) 388-398.  
590 doi:10.1016/j.ejps.2011.09.006
- 591 [20] Y. Wu, W. Yang, C. Wang, J. Hu, S. Fu, *Int. J. Pharm.* 295 (2005) 235-245.  
592 doi:10.1016/j.ijpharm.2005.01.042
- 593 [21] Y. Jeong, D. Kim, M. Jang, J. Nah, *Carbohydr. Res.* 343 (2008) 282-289.  
594 doi:10.1016/j.carres.2007.10.025
- 595 [22] U. Termsarasab, I. Yoon, J. Park, H.T. Moon, H. Cho, D. Kim, *Int. J. Pharm.* 464 (2014)  
596 127-134. <http://dx.doi.org/10.1016/j.ijpharm.2014.01.015>
- 597 [23] E.V. Batrakova, A.V. Kabanov, *J. Control. Release* 130 (2008) 98-106.  
598 doi:10.1016/j.jconrel.2008.04.013
- 599 [24] E.V. Batrakova, S. Li, A.M. Brynskikh, A.K. Sharma, Y. Li, M. Boska, N. Gong, R.L.  
600 Mosley, V.Y. Alakhov, H.E. Gendelman, A.V. Kabanov, *J. Control. Release* 143 (2010) 290-  
601 301. doi:10.1016/j.jconrel.2010.01.004
- 602 [25] Y. Zhao, C. Sun, C. Lu, D. Dai, H. Lv, Y. Wu, C. Wan, L. Chen, M. Lin, X. Li, *Cancer*  
603 *Lett.* 311 (2011) 187-194. doi:10.1016/j.canlet.2011.07.013
- 604 [26] Y. Chen, W. Zhang, Y. Huang, F. Gao, X. Sha, X. Fang, *Int. J. Pharm.* 488 (2015) 44-58.  
605 <http://dx.doi.org/10.1016/j.ijpharm.2015.04.048>
- 606 [27] L. Sanchez, M. Mitjans, M.R. Infante, M.P. Vinardell, *Toxicol. Lett.* 161 (2006) 53-60.  
607 doi:10.1016/j.toxlet.2005.07.015
- 608 [28] L. Sanchez, M. Mitjans, M.R. Infante, M.T. García, M.A. Manresa, M.P. Vinardell, *Amino*  
609 *Acids* 32 (2007) 133-136. PMID: 16729197
- 610 [29] M.A. Vives, M.R. Infante, E. Garcia, C. Selve, M. Maugras, M.P. Vinardell, *Chem. Biol.*  
611 *Interact.* 118 (1999) 1-18. PII: S0009-2797(98)00111-2

- 612 [30] P. Calvo, C. Remuñán-López, J.L. Vila-Jato, M.J. Alonso, *J. Appl. Polym. Sci.* 63 (1997)  
613 125-132. [doi:10.1023/A:1012128907225](https://doi.org/10.1023/A:1012128907225)
- 614 [31] Q. Gan, T. Wang, C. Cochrane, P. McCarron, *Colloids Surf. B: Biointerfaces* 44 (2005)  
615 65-73. [doi:10.1016/j.colsurfb.2005.06.001](https://doi.org/10.1016/j.colsurfb.2005.06.001)
- 616 [32] S.S. Santos, A. Lorenzoni, N.S. Pegoraro, L.B. Denardi, S.H. Alves, S.R. Schaffazick, L.  
617 Cruz, *Colloids Surf. B: Biointerfaces* 116 (2014) 270-276.  
618 <http://dx.doi.org/10.1016/j.colsurfb.2014.01.011>
- 619 [33] M.C. Fontana, A. Beckenkamp, A. Buffon, R.C.R. Beck, *Int. J. Nanomed.* 9 (2014) 2979-  
620 2991. <http://dx.doi.org/10.2147/IJN.S62857>
- 621 [34] R.W. Kormeyer, R. Gumy, E. Doelker, P. Buri, N.A. Peppas, *Int. J. Pharm.* 15 (1983) 25-  
622 35. [doi:10.1016/0378-5173\(83\)90064-9](https://doi.org/10.1016/0378-5173(83)90064-9)
- 623 [35] P.L. Ritger, N.A. Peppas, *J. Control. Release* 5 (1987) 23-36. [doi:10.1016/0168-  
624 3659\(87\)90034-4](https://doi.org/10.1016/0168-3659(87)90034-4)
- 625 [36] N.A. Peppas, J.J. Sahlin, *Int. J. Pharm.* 57 (1989) 169-172. [doi:10.1016/0378-  
626 5173\(89\)90306-2](https://doi.org/10.1016/0378-5173(89)90306-2)
- 627 [37] P. Rosa, A.P.S. Salla, C.B. Silva, C.M.B. Rolim, A.I.H. Adams, *AAPS PharmSciTech* 15  
628 (2014) 1155-1162. doi: 10.1208/s12249-014-0149-0
- 629 [38] W. Tiyaboonchai, *Naresuan University Journal* 11 (2003) 51-66.
- 630 [39] T. Kean, M. Thanou, *Adv. Drug Deliv. Rev.* 62 (2010) 3-11.  
631 [doi:10.1016/j.addr.2009.09.004](https://doi.org/10.1016/j.addr.2009.09.004)
- 632 [40] D. Lee, K. Powers, R. Baney, *Carbohydr. Polym.* 58 (2004) 371-377.  
633 [doi:10.1016/j.carbpol.2004.06.033](https://doi.org/10.1016/j.carbpol.2004.06.033)
- 634 [42] L. Keawchaon, R. Yoksan, *Colloids Surf. B: Biointerfaces* 84 (2011) 163-171.  
635 [doi:10.1016/j.colsurfb.2010.12.031](https://doi.org/10.1016/j.colsurfb.2010.12.031)
- 636 [42] M.R. Avadi, A.M.M.Sadeghi, N. Mohammadpour, S. Abedin, F. Atyabi, R. Dinarvand, M.  
637 Rafiee-Tehrani, *Nanomedicine: Nanotechnol., Biol., Med.* 6 (2010) 58-63.  
638 [doi:10.1016/j.nano.2009.04.007](https://doi.org/10.1016/j.nano.2009.04.007)
- 639 [43] Q. Gan, T. Wang, *Colloids Surf. B: Biointerfaces* 59 (2007) 24-34.  
640 [doi:10.1016/j.colsurfb.2007.04.009](https://doi.org/10.1016/j.colsurfb.2007.04.009)
- 641 [44] D.R. Nogueira, L. Tavano, M. Mitjans, L. Pérez, M. R. *Biomaterials* 34 (2013) 2758-2772.  
642 <http://dx.doi.org/10.1016/j.biomaterials.2013.01.005>

- 643 [45] S. Mao, W. Sun, T. Kissel, *Adv. Drug Deliv. Rev.* 62 (2010) 12-27.  
644 doi:10.1016/j.addr.2009.08.004
- 645 [46] L. Tavano, R. Aiello, G. Ioele, N. Picci, R. Muzzalupo, *Colloids Surf. B: Biointerfaces* 118  
646 (2014) 7-13. doi: 10.1016/j.colsurfb.2014.03.016.
- 647 [47] M. Xu, J. Qian, X. Liu, T. Liu, H. Wang, *Mat. Sci. Eng. C* 50 (2015) 341-347.  
648 <http://dx.doi.org/10.1016/j.msec.2015.01.098>
- 649 [48] S.S. Kim, Y.M. Lee, *Polymer* 36 (1995) 4497-4501. doi:10.1016/0032-3861(95)96859-7
- 650 [49] H. Hosseinzadeh, F. Atyabi, R. Dinarvand, S.N. Ostad, *Int. J. Nanomed.* 7 (2012) 1851-  
651 1863. <http://dx.doi.org/10.2147/IJN.S26365>
- 652 [50] S. Danson, D. Ferry, V. Alakhov, J. Margison, D. Kerr, D. Jowle, M. Brampton, G. Halbert,  
653 M. Ranson, *Br. J. Cancer.* 90 (2004) 2085-2091. doi: 10.1038/sj.bjc.6601856
- 654 [51] Y. Jin, H. Hu, M. Qiao, J. Zhu, J. Qi, C. Hu, Q. Zhang, D. Chen, *Colloids Surf. B*  
655 *Biointerfaces* 94 (2012) 184– 191. doi:10.1016/j.colsurfb.2012.01.032
- 656 [52] J. Ji, S. Hao, D. Wu, R. Huang, Y. Xu, *Carbohydr. Polym.* 85 (2011) 803-808.  
657 doi:10.1016/j.carbpol.2011.03.051
- 658 [53] J. Park, P.M. Fong, J. Lu, K.S. Russell, C.J. Booth, W.M. Saltzman, T.M. Fahmy.  
659 *Nanomed. Nanotechnol.* 5 (2009) 410-418. doi:10.1016/j.nano.2009.02.002
- 660 [54] D.B. Leeper, K. Engin, A.J. Thistlethwaite, H.D. Hitchon, J.D. Dover, D.Li, L. Tupchong,  
661 *Int. J. Radiation Oncology Biol. Phys.* 28 (1994) 935-943. doi:10.1016/0360-3016(94)90114-7
- 662 [55] F. Yan, C. Zhang, Y. Zheng, L. Mei, L. Tang, C. Song, H. Sun, L. Huang, *Nanomedicine:*  
663 *Nanotechnol., Biol., Med.* 6 (2010) 170-178. doi:10.1016/j.nano.2009.05.004
- 664 [56] L. Mei, Y. Zhang, Y. Zheng, G. Tian, C. Song, D. Yang, H. Chen, H. Sun, Y. Tian, K. Liu,  
665 Z. Li, L. Huang, *Nanoscale Res. Lett.* 4 (2009) 1530-1539. doi: 10.1007/s11671-009-9431-6
- 666 [57] R.S.T. Aydin, M. Pulat, *J. Nanomater.* 2012 (2012) 1-10. doi:10.1155/2012/313961
- 667 [58] S.A. Agnihotri, N.N. Mallikarjuna, T.M. Aminabhavi, *J. Control. Release* 100 (2004) 5-  
668 28. doi:10.1016/j.jconrel.2004.08.010
- 669 [59] P.L. Ritger, N.A. Peppas, *J. Control. Release* 5 (1987) 37-42. doi:10.1016/0168-  
670 3659(87)90035-6
- 671 [60] M. Fazil, S. Md, S. Haque, M. Kumar, S. Baboota, J. Sahni, J. Ali, *Eur. J. Pharm. Sci.* 47  
672 (2012) 6-15. <http://dx.doi.org/10.1016/j.ejps.2012.04.013>
- 673 [61] J.C. Kasper, G. Winter, W. Friess, *Eur. J. Pharm. Biopharm.* 85 (2013) 162-169.  
674 <http://dx.doi.org/10.1016/j.ejpb.2013.05.019>

- 675 [62] M.K. Lee, M.Y. Kim, S. Kim, J. Lee, J. Pharm. Sci. 98 (2009) 4808-4817.  
676 doi:10.1002/jps.21786
- 677 [63] A. Rampino, M. Borgogna, P. Blasi, B. Bellich, A. Cesàro, Int. J. Pharm. 455 (2013) 219-  
678 228. <http://dx.doi.org/10.1016/j.ijpharm.2013.07.034>
- 679 [64] T. Cerchiara, A. Abruzzo, M. di Cagno, F. Bigucci, A. Bauer-Brandl, C. Parolin, B. Vitali,  
680 M.C. Gallucci, B. Luppi, Eur. J. Pharm. Biopharm. 92 (2015) 112-119.  
681 <http://dx.doi.org/10.1016/j.ejpb.2015.03.004>
- 682 [65] F. Yan, C. Zhang, Y. Zheng, L. Mei, L. Tang, C. Song, H. Sun, L. Huang. Nanomedicine:  
683 Nanotechnol., Biol., Med. 6 (2010) 170-178. doi:10.1016/j.nano.2009.05.004
- 684 [66] R.M. Silverstein, F.X. Webster, D.J. Kiemle, Spectrometric Identification of Organic  
685 Compounds, 7th Edition, John Wiley & Sons, 2005.
- 686 [67] M. Luangtana-anan, S. Limmatvapirat J. Nunthanid, R. Chalongsuk, K. Yamamoto, AAPS  
687 PharmSciTech 11 (2010) 1376-1382. doi: 10.1208/s12249-010-9512-y
- 688

689 **Figure captions:**

690 **Fig. 1.** Design of pH-responsive DOX-loaded CS-NPs to facilitate target drug release at the  
691 tumor site.

692 **Fig. 2.** UV-Vis absorption spectra of the DOX extracted from NPs (A) and DOX aqueous  
693 solution (B).

694 **Fig. 3.** pH-dependent *in vitro* cumulative DOX release from NPs in PBS buffer at pH 7.4, 6.6  
695 and 5.4. (A) DOX-CS-NPs, (B) PEG-DOX-CS-NPs, (C) Polox-DOX-CS-NPs and (D) DOX-  
696 CS-NPs without 77KS. Results are expressed as the mean  $\pm$  SE of three independent  
697 experiments. Statistical analyses were performed using ANOVA followed by Tukey's multiple  
698 comparison test. <sup>a</sup> Significant difference from PBS pH 7.4 ( $p < 0.05$ ), <sup>b</sup> highly significant  
699 difference from PBS pH 7.4 ( $p < 0.01$ ).

700 **Fig. 4.** FT-IR spectra of pure DOX (A), CS raw material (B), Polox-DOX-CS-NPS (C) and  
701 Poloxamer 188 (D).

702 **Fig. 5.** FT-IR spectra of 77KS (A), DOX-CS-NPs (B), DOX-CS-NPs without 77KS (C) and  
703 PEG-DOX-CS-NPs (D).

704 **Fig. 6.** *In vitro* antitumor activity of unloaded-CS-NPs, free DOX and DOX-loaded CS-NPs in  
705 HeLa cell line.

706

**Table 1.** Characterization of unloaded and DOX-loaded CS-NPs with or without 77KS. The lyophilized NPs (L-NPs) were analyzed after redispersion in ultra-pure water.

Sample	Particle size (nm) $\pm$ SD*	Polydispersity index $\pm$ SD*	Zeta potential (mV) $\pm$ SD*	pH	EE% $\pm$ SD*
CS-NPs (CS:TPP)	170.30 $\pm$ 0.84	0.19 $\pm$ 0.02	25.20 $\pm$ 1.87	5.66	-
DOX-CS-NPs (CS:TPP)	190.35 $\pm$ 1.70	0.22 $\pm$ 0.01	21.90 $\pm$ 1.12	5.70	75.54 $\pm$ 4.98
CS-NPs	176.77 $\pm$ 1.79	0.20 $\pm$ 0.02	24.00 $\pm$ 1.82	5.66	-
DOX-CS-NPs	197.50 $\pm$ 2.30	0.22 $\pm$ 0.01	21.70 $\pm$ 0.81	5.72	66.50 $\pm$ 2.68
PEG-CS-NPs	211.10 $\pm$ 1.55	0.24 $\pm$ 0.01	23.30 $\pm$ 1.96	4.68	-
PEG-DOX-CS-NPs	226.40 $\pm$ 2.33	0.23 $\pm$ 0.01	23.65 $\pm$ 1.06	5.19	66.32 $\pm$ 3.54
Polox-CS-NPs	184.50 $\pm$ 2.00	0.21 $\pm$ 0.02	22.05 $\pm$ 0.91	5.48	-
Polox-DOX-CS-NPs	209.70 $\pm$ 1.35	0.22 $\pm$ 0.03	21.00 $\pm$ 0.85	5.60	62.21 $\pm$ 2.88
L-DOX-CS-NPs	217.45 $\pm$ 4.49	0.33 $\pm$ 0.02	12.40 $\pm$ 0.15	6.14	67.42 $\pm$ 10.85
L-PEG-DOX-CS-NPs	491.60 $\pm$ 32.38	0.73 $\pm$ 0.09	20.45 $\pm$ 0.78	5.91	65.32 $\pm$ 3.18
L-Polox-DOX-CS-NPs	252.80 $\pm$ 7.46	0.40 $\pm$ 0.03	17.50 $\pm$ 0.93	5.98	61.27 $\pm$ 2.28

709

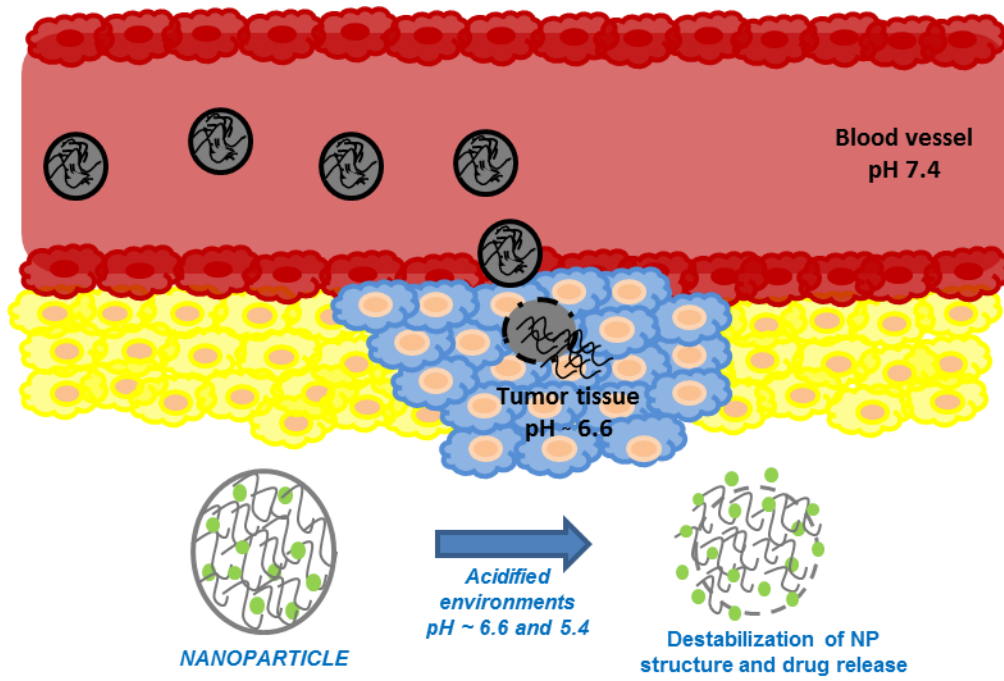
710

711 **Table 2.** Observed rate constants, correlation coefficients, MSC and half-lives ( $t_{1/2}$ ) obtained by  
 712 mathematical modeling of DOX release from the different NPs when immersed in PBS buffer at  
 713 pH 7.4, 6.6 and 5.4. Results are expressed as mean  $\pm$  standard deviation (SD) of three  
 714 experiments.

	pH medium	DOX-CS-NPs	PEG-DOX-CS-NPs	Polox-DOX-CS-NPs
Biexponential				
$r$		0.99 $\pm$ 0.01	1.00 $\pm$ 0.01	1.00 $\pm$ 0.01
MSC		3.96 $\pm$ 0.36	4.28 $\pm$ 0.25	4.17 $\pm$ 0.45
$k_1$ (h <sup>-1</sup> )		0.44 $\pm$ 0.05	0.67 $\pm$ 0.07	2.84 $\pm$ 1.25
$t_{1/2} k_1$ (h <sup>-1</sup> )	7.4	1.58 $\pm$ 0.47	1.02 $\pm$ 0.29	0.24 $\pm$ 0.09
$k_2$ (h <sup>-1</sup> )		0.002 $\pm$ 0.01	0.01 $\pm$ 0.01	0.36 $\pm$ 0.36
$t_{1/2} k_2$ (h <sup>-1</sup> )		407.64 $\pm$ 33.76	93.64 $\pm$ 9.12	1.91 $\pm$ 0.38
$a$		0.74 $\pm$ 0.04	0.70 $\pm$ 0.03	0.31 $\pm$ 0.08
$b$		0.23 $\pm$ 0.04	0.26 $\pm$ 0.02	0.68 $\pm$ 0.08
Monoexponential				
$r$		0.99 $\pm$ 0.01	0.99 $\pm$ 0.01	0.98 $\pm$ 0.01
MSC	6.6	3.74 $\pm$ 0.32	3.46 $\pm$ 0.63	3.13 $\pm$ 0.35
$k$ (h <sup>-1</sup> )		0.64 $\pm$ 0.04	1.23 $\pm$ 0.08	1.05 $\pm$ 0.08
$t_{1/2}$ (h <sup>-1</sup> )		1.07 $\pm$ 0.05	0.56 $\pm$ 0.03	0.65 $\pm$ 0.14
$r$		1.00 $\pm$ 0.01	0.99 $\pm$ 0.01	1.00 $\pm$ 0.00
MSC	5.4	4.68 $\pm$ 0.29	3.31 $\pm$ 0.31	5.07 $\pm$ 0.25
$k$ (h <sup>-1</sup> )		0.76 $\pm$ 0.03	0.98 $\pm$ 0.07	0.91 $\pm$ 0.03
$t_{1/2}$ (h <sup>-1</sup> )		0.90 $\pm$ 0.10	0.71 $\pm$ 0.20	0.76 $\pm$ 0.19

716

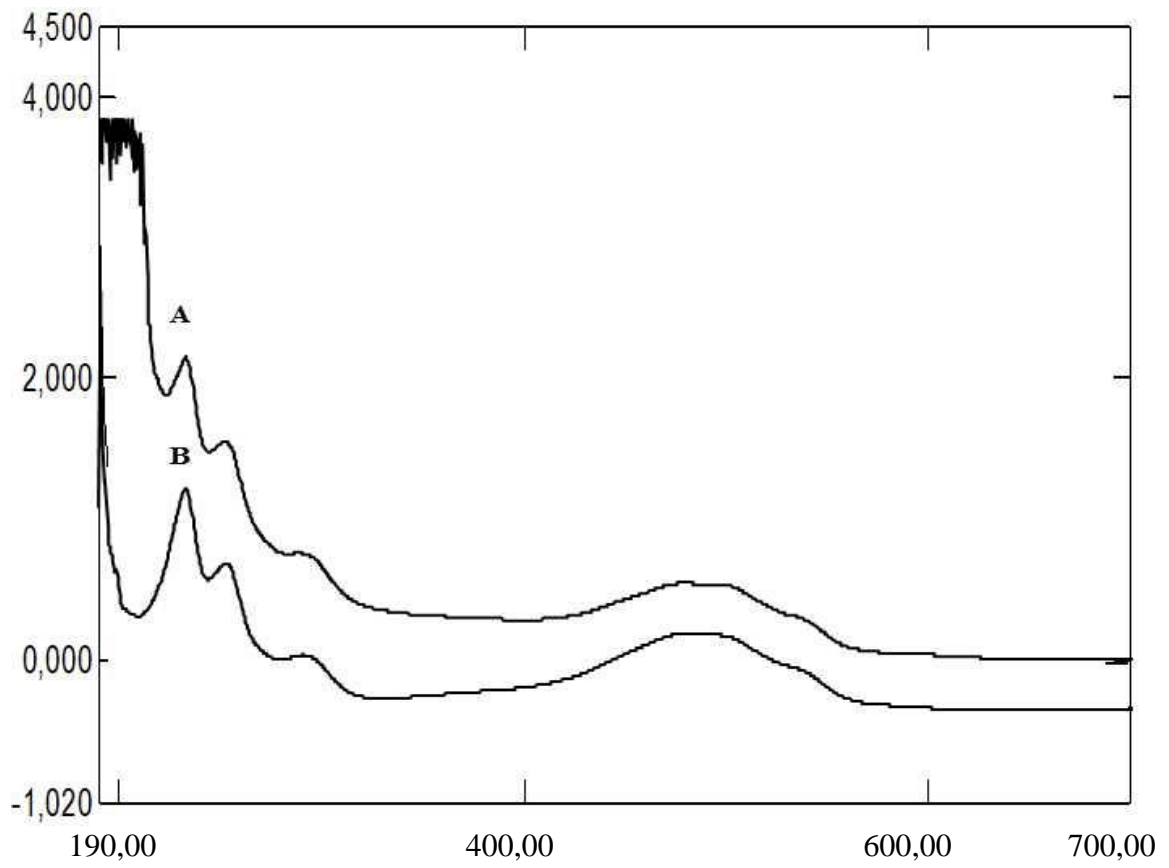
717 Fig 1



718

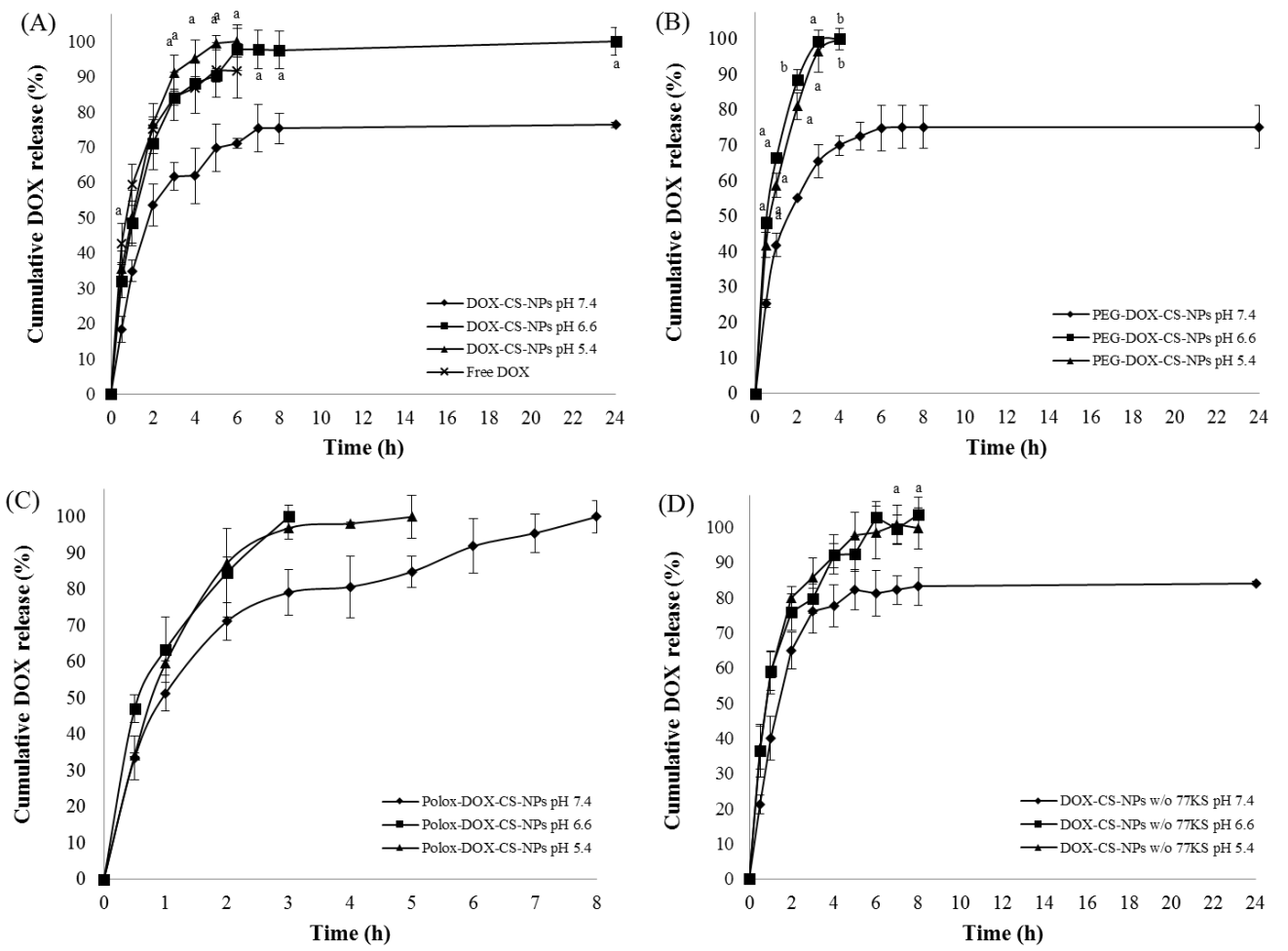
719

720 Fig 2



721

722

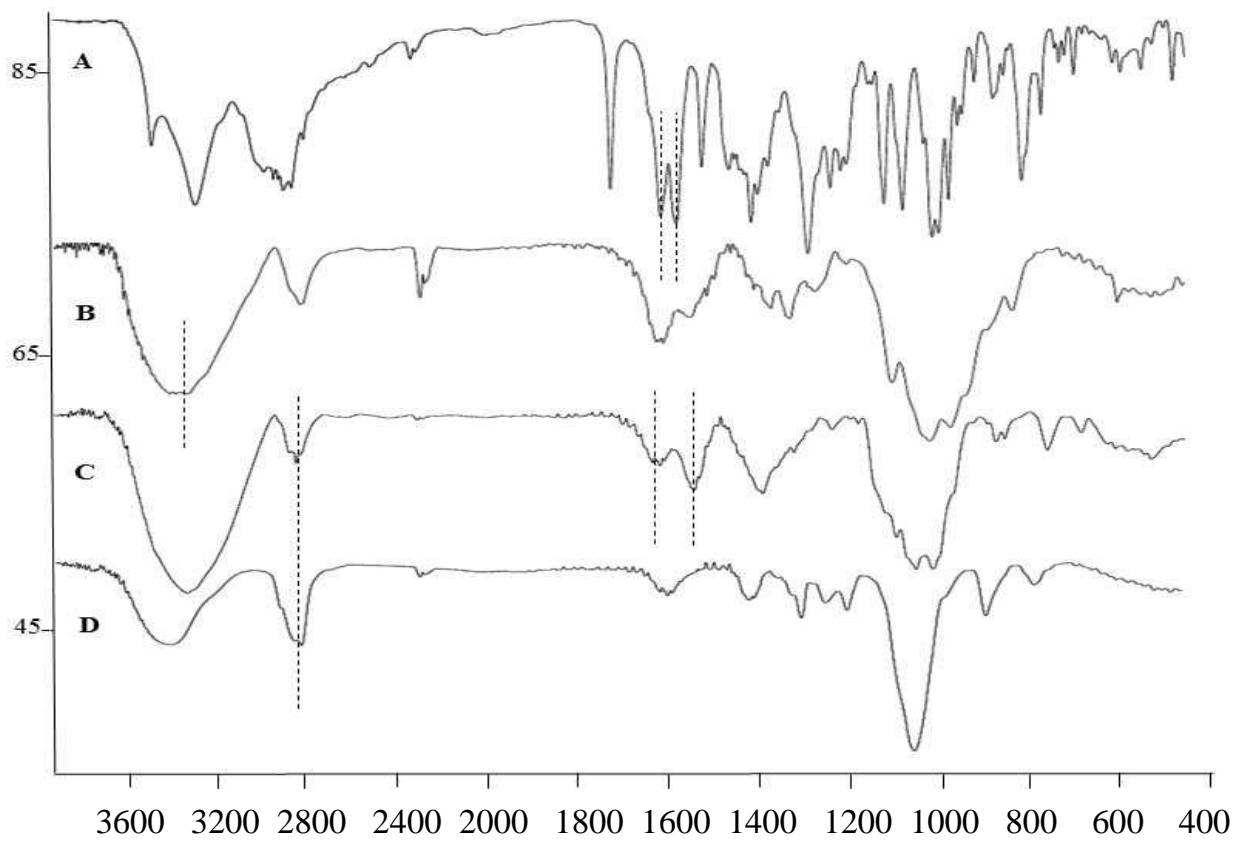


724

725

726 Fig. 4

727



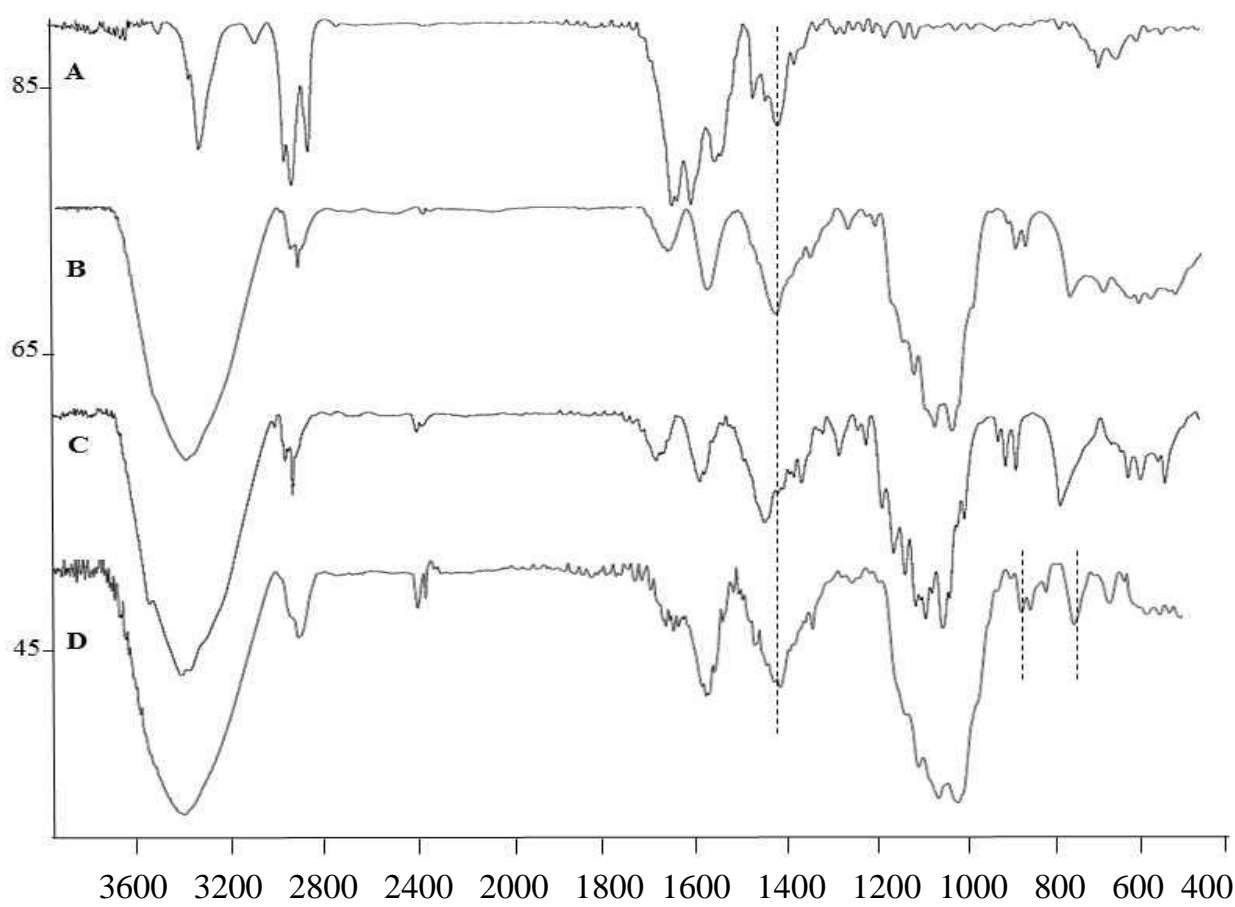
728

729

730

**Wavenumber [1cm<sup>-1</sup>]**

731 Fig 5



732

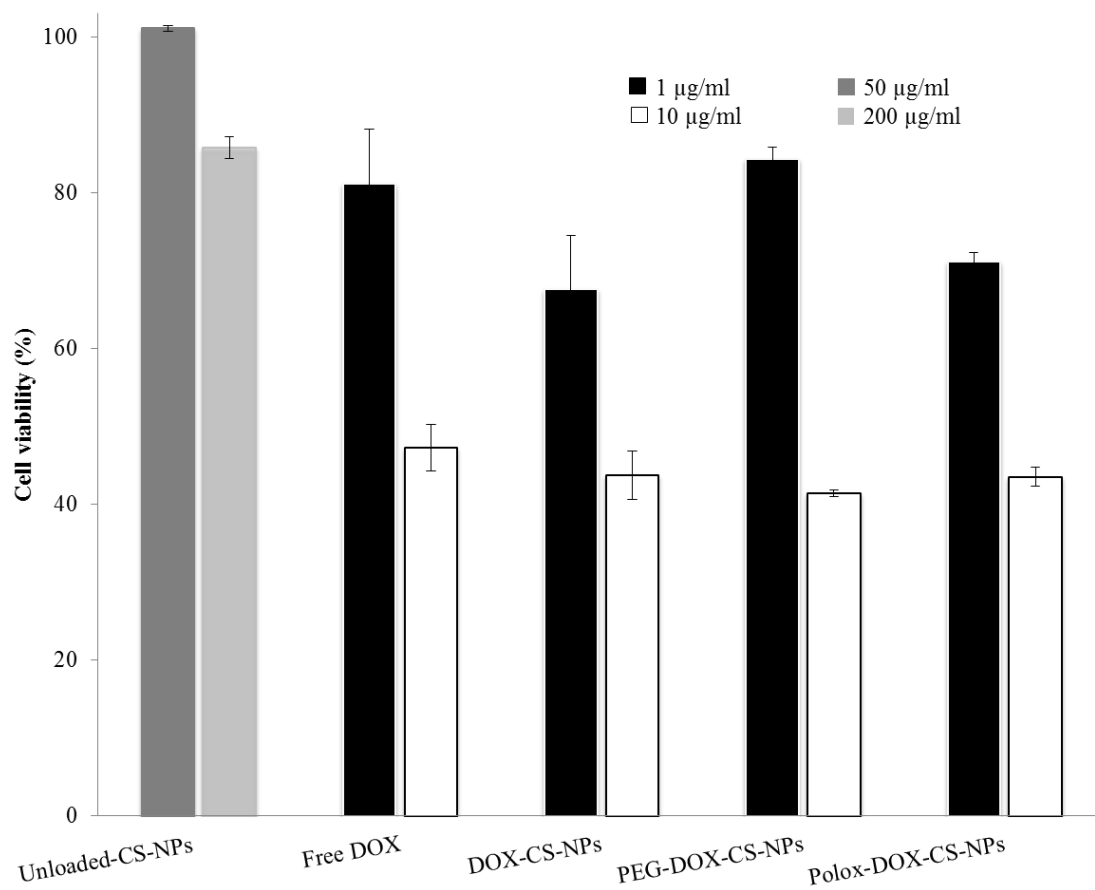
733

734

**Wavenumber [ $\text{cm}^{-1}$ ]**

735 Fig 6

736



737